Preprint Title Bioactive specialized metabolites produced by the emerging pathogen *Diplodia olivarum*

Authors Roberta Di Lecce, Marco Masi, Benedetto T. Linaldeddu, Gennaro Pescitelli, Lucia Maddau and Antonio Evidente

Publication Date 14 Sep. 2020

Article Type Full Research Paper

Supporting Information File 1 Supporting Information.docx; 682.7 KB

ORCID® iDs Marco Masi - https://orcid.org/0000-0003-0609-8902; Benedetto T. Linaldeddu - https://orcid.org/0000-0003-2428-9905; Gennaro Pescitelli - https://orcid.org/0000-0002-0869-5076; Lucia Maddau - https://orcid.org/0000-0002-8158-8242; Antonio Evidente - https://orcid.org/0000-0001-9110-1656

Bioactive specialized metabolites produced by the emerging pathogen *Diplodia olivarum*

Roberta Di Lecce,[1] Marco Masi,[1,*] Benedetto Teodoro Linaldeddu,[2] Gennaro Pescitelli,[3] Lucia Maddau,[4] Antonio Evidente[1]

[1]Dipartimento di Scienze Chimiche, Università di Napoli Federico II, Complesso Universitario Monte Sant'Angelo, Via Cintia 4, 80126, Napoli, Italy.

[2]Dipartimento Territorio e Sistemi Agro-Forestali, Università di Padova, Viale dell'Università 16, Legnaro 35020, Italy

[3]Dipartimento di Chimica e Chimica Industriale, Università di Pisa, Via Moruzzi 3, 56124 Pisa, Italy

[4]Dipartimento di Agraria, Sezione di Patologia Vegetale ed Entomologia, Università degli Studi di Sassari, Viale Italia 39, 07100, Sassari, Italy

*Corresponding author

E-mail address: marco.masi@unina.it

Abstract

A new cleistanthane *nor*-diterpenoid, named olicleistanone (**1**), was isolated as a racemate from the culture filtrates of *Diplodia olivarum* an emerging pathogen involved in the aetiology of branch canker and dieback of in several plant species typical of the Mediterranean maquis in Sardinia, Italy. When the fungus was grown *in vitro* on Czapek medium olicleistanone was isolated together with some already known phytotoxic diterpenoids identified as sphaeropsidins A, C, and G and diplopimarane (**2**-**5**). Olicleistanone was characterized by spectroscopic methods (essentially 1D and 2D NMR and HR ESIMS) as 4-ethoxy-6a-methoxy-3,8,8-trimethyl-4,5,8,9,10,11-hexahydrodibenzo[*de,g*]chromen-7(6a*H*)-one. When the fungus was grown on mineral salt medium showed to produce (-)-mellein (**6**), sphaeropsidin A and a very low amount of sphaeropsidin G and diplopimarane. Olicleistanone (**1**) exhibited remarkable activity against *Artemia salina* L. (100% larval mortality) at 100 µg/mL. In addition, it did not exhibit phytotoxic, antifungal and antioomycetes activity. Among the metabolites isolated (**1**-**6**), the sphaeropsindin A (**2**) proved to be active in all bioassay performed exhibiting remarkable phytotoxicity on *Phaseolus vulgaris* L., *Juglans regia* L. and *Quercus suber* L. leaves at 1 mg/mL. Moreover, it completely inhibited the mycelial growth of *Athelia rolfsii, Diplodia corticola, Phytophthora cambivora* and *P. lacustris* at 200 µg/plug. It was also active in the *Artemia salina* assay. In this latter assay, diplopimarane (**4**) and sphaeropsidin G (**4**) were active (100% larval mortality). Diplopimarane also showed antifungal and antioomycetes activities. *Athelia rolfsii* was the most sensitive species to diplopimarane. Sphaeropsidin C (**3**) and (-)-mellein (**6**) were found to be inactive in all bioassays. Results obtained in this study have allowed us to expand the knowledge on the metabolic profile of *Botryosphaeriaceae* members and characterize the main secondary metabolites secreted *in vitro* by *D. olivarum* for the first time.

Keywords**:** *Botryosphaeriaceae*, emerging diseases, forest ecosystems, olicleistanone, toxins

Introduction

Diplodia Fr. is a large genus in the family *Botryosphaeriaceae* typified by *Diplodia mutila* (Fr.: Fr.) Fr. [1]. Species of *Diplodia* are cosmopolitan in temperate and subtropical regions and occur on a wide range of angiosperm and gymnosperm hosts [2]. They exhibit diverse life-styles spanning from endophytes able to inhabit different asymptomatic plant tissues to aggressive pathogens that cause severe diseases in various plant hosts [2-5]. The increasing number of reports of new diseases caused by these pathogens during the last decades has stimulated the research into the virulence factors involved in the pathogenesis process. This allowed several bioactive secondary metabolites to be isolated and identified belonging to different classes of organic compounds such as pimarane diterpenoids, α-pyrones, furanones, diplobifuranylones, naphthoquinones, biphenols, cyclohexene oxides, furopyrans, isochromanones and melleins from the emerging pathogens *Diplodia africana, Diplodia corticola, Diplodia cupressi, Diplodia fraxini, Diplodia quercivora* and *Diplodia sapinea* [2,6]. It has been shown that some phytotoxins produced by *Diplodia* species such as the tetracyclic pimarane diterpenoid sphaeropsidin A have a broad-spectrum of biological activities including anti-drug-resistant cancer cells by targeting regulatory volume increase [2]. Recently, another species namely *Diplodia olivarum* has been emerging as an aggressive pathogen on different plant hosts in Italy. *D. olivarum* was originally found on rotting olive drupes in southern Italy and described as a new species in 2008 [7]. It was later reported as a canker agent on carob tree [8], lentisk [9] and wild olive [10]. Symptoms of the disease in infected hosts include sunken cankers with characteristic wedge-shaped wood necrosis on branches and stem. Foliar symptoms have also been observed especially on lentisk shoots (Figure 1).

Therefore, given the growing expansion of severe dieback caused by *D. olivarum* in several natural ecosystem in Italy, and the still limited information available about the bioactive specialized metabolites produced by this emerging pathogen, a study was conducted to isolate, identify and evaluate the phytotoxic, antifungal, antioomycetes and zootoxic activities of the main compounds produced *in vitro*.

Results and discussion

The organic extract obtained from *D. olivarum* culture filtrates grown on Czapek medium was purified as detailed in the Materials and methods section to yield a new *nor*-diterpenoid cleistanthane (**1**; Figure 2), named olicleistanone, together with four known pimarane diterpenoids identified as sphaeropsidins A, C, and G and diplopimarane (**2-5**; Figure 2). When the fungus was grown on mineral salt medium showed to produce (-)-mellein (**6**; Figure 2), sphaeropsidin A (**2**) and very low amount of sphaeropsidin G (**4**) and diplopimarane (**5**). The known compounds (**2**-**6**) were identified comparing their physical (specific optical rotation) and spectroscopic data (^{1}H NMR and ESIMS) with those reported in literature [2,11-18].

Olicleistanone (**1**) has a molecular formula of $C_{22}H_{28}O_4$ as deduced from its HR ESIMS spectrum and consistent with nine hydrogen deficiencies. Preliminary investigation of its ^{1}H and ^{13}C NMR spectra (Table 1) showed that it is close related to a tricyclic *nor*-diterpenoid, with aromatized and cyclohexadiene rings (A and B) joined to a dihydropyran ring (D) generated probably from a cleistanthane carbon skeleton [19]. The signal at δ 195.5 in the ^{13}C NMR spectrum also suggested the presence of a conjugated ketone group [20]. These results are in full agreement with the bands typical for carbonyl and aromatic groups observed in the IR spectrum [21] and the absorption maxima observed in the UV spectrum [22].

In particular, its ^{1}H and COSY spectra [23] showed the presence of two doublets (J = 7.9 Hz) at δ 7.31 and 7.18, typical signals of two *ortho*-coupled protons (H-11 and H-12) of a 1,2,3,4-tetrasubstituted C benzene ring. The same spectra showed the singlets of a methoxy group (CH_3-22), a vinyl methyl (CH_3-17) and two methyls (CH_3-18 and CH_3-19) bonded to a quaternary carbon at δ 3.38, 2.34, and 1.36 and 1.23, respectively. The latter two represent the head of the geranylgeranyl biosynthetic precursor which generated the diterpenoid cleistanthane carbon skeleton. The same spectra showed the signal of an ethoxy group with the protons of the

oxygenated methylene (CH_2-20) resonating as two double quartets (J = 14.2 and 7.0 Hz) at δ 3.64 and 3.33 being coupled with the terminal methyl (CH_3-21) which appeared as a triplet (J = 7.0 Hz) at δ 1.14. A signal pattern due to pyran moiety (ring D) of the benzopyran system (C-D rings) appeared as ABC system with a doublet (J = 12.7 Hz), a double doublet (J = 12.7 and 3.3 Hz) (the signal of CH_2-16) and a doublet (J = 3.3 Hz) (CH-15) at δ 4.41, 4.22 and 4.20 with the last two signals in part overlapped. Finally, the spectra showed the signal typical of the three adjacent methylene groups (CH_2-1, CH_2-2 and CH_2-3) of the A ring. In fact, a double triplet (J = 18.8 and 6.1 Hz) and a doublet of double doublets (J = 18.8, 12.2 and 6.6 Hz) due to the protons of CH_2-1 were observed at δ 2.77 and 2.47, while the protons of the other two adjacent methylene groups appeared as complex multiplets at δ 1.80 (CH_2-2), and 1.62 and 1.49 (CH_2-3), respectively [22].

The correlations observed in the HSQC spectrum [23] (Table 1) allowed the chemical shifts to be assigned to the protonated carbons. In particular, the signals at δ 131.3, 125.0, 69.5, 60.5, 59.0, 55.7, 40.5, 29.7, 27.7, 27.4, 18.6, 18.4 and 15.4 were assigned to C-12, C-11, C-15, C-16, C-20, C-22, C-3, C-19, C-18, C-1, C-2, C-17, and C-21, respectively [20].

The long range couplings observed in the HMBC spectrum [23] (Table 1) allowed the quaternary carbons to be assigned. The signals at δ 34.0 correlated with H_2-1, H_2-2, H_3-18 and H_3-19, 136.4 with H_2-1, H_2-3, H_3-18 and H_3-19, 195.5 with H_2-1, 92.3 with H-15, H_2-16 and H-20A, 130.6 with H-12 and H_3-17, 146.1 with H_2-1, H_2-2, H-11, 138.7 with H-11 and H_3-17, 130.2 with H-12, H-15 and H_2-16 and were assigned to C-4, C-5, C-6, C-7, C-8, C-10, C-13 and C-14 respectively. The resulting signal at δ 132.9 was assigned to C-9 [20]. Furthermore, the correlation between C-7 and H-20A allowed the ethoxy group to be located at C-7 and consequently the methoxy group at C-15.

Thus the chemical shifts were assigned to all the carbons and the corresponding protons, which are reported in Table 1, and olicleistanone (**1**) was formulated as 4-ethoxy-6a-methoxy-3,8,8-trimethyl-4,5,8,9,10,11-hexahydrodibenzo[*de,g*]chromen-7(6a*H*)-one.

The structure assigned to **1** were supported by the other HMBC couplings reported in Table 1 and from the data of its HR ESIMS spectrum which showed the sodium dimer $[2M+Na]^+$, the potassium $[M+K]^+$ and the sodium $[M+Na]^+$ adducts at *m/z*: 735, 395, 379.1876. The significant ion $[M+H-CH_3CH_2OH]^+$ observed at *m/z* 311 was probably generated from a pseudo-molecular ion by loss of ethanol.

Attempts to assign the relative configuration of **1** were made recording a NOESY spectrum. The measured NOESY correlations are reported in Table 2 but since there is no clear correlation between the protons of the methoxy and ethoxy groups, these data alone were not enough to assign the relative configuration of the two chiral centres (C-7 and C-15). In order to better interpret NMR data, a molecular modelling study was undertaken. First, two diastereomeric structures (7*S*,15*S*)-**1** and (7*S*,15*R*)-**1** were generated and their possible conformations were explored by means of a conformational search with molecular mechanics (molecular Merck force field, MMFF). Geometry optimizations were then run with the density functional method (DFT) at the B97M-V/6-311+G(2df,2p)//B3LYP/6-31G(d) level, using the computational protocol developed by Hehre et al. for the prediction of ^{13}C chemical shifts of flexible compounds [24]. For the two diastereomers, 6 or 10 conformers were found with detectable populations at room temperature. The various conformers differed in the conformation of the methoxy and ethoxy groups, but also in the puckering of ring A. A clear difference between the two diastereomers was the orientation of H-15, which was predominantly pseudo-equatorial in (7*S*,15*S*)-**1** and pseudo-axial (7*S*,15*R*)-**1**. Thus, we thought that the coupling constants between H-15 and H-16a/H-16b could be used to discriminate between the two isomers. Experimentally, H-15 appears as a doublet with splitting of 3.3 Hz, meaning that one $J_{15/16}$ was small (3.3 Hz) and the other one negligible. This fact was in accordance with a pseudo-equatorial orientation. $^3J_{15/16}$ were then estimated with two different methods, namely a Karplus curve and spin-spin coupling calculations at B3LYP/pcJ-0 level. The results are shown in Table 3 and strongly support the assignment of **1** as (7*S**,15*S**)-**1**. Finally, ^{13}C- NMR calculations were run at the B3LYP/6-31G(d) level. The estimated rms (root-mean-square) error between

experimental and calculated ^{13}C chemical shifts was acceptable (2.4-2.5) but similar for both isomers, thus confirming the above assignment but without further supporting it. Anyway, we believe that our argument based on *J*-couplings is accurate enough to assign the relative configuration.

Coming to the absolute configuration, we measured the ECD spectrum of a solution of **1** in acetonitrile (1 mM, 0.01 cm cell). To our surprise, the ECD spectrum was not distinguishable from the baseline over the whole range (185-400 nm, data not shown), despite the optimal absorption (0.3 to 0.8 for the absorption peaks). We must conclude that the isolated sample of **1** was a racemate. Racemic natural products are rare but sometimes encountered and are thought to be the result of nonenzymatic reactions [25]. We noticed that the chirality center at C-7 of **1** is a tertiary benzylic carbon in α position to carbonyl group; however, racemization of this centre does not occur in a post-synthetic step, otherwise one would obtain a couple of diastereomers. On the other hand, the isolated (7*S*,15*S*)-**1** isomer is more stable than its (7*S*,15*R*) diastereomer by about 2 kcal/mol at our level of calculation, suggesting that if the chiral center at C-15 is biosynthesized in a later step than C-7, its configuration would be dictated by that at C-7.

All isolated metabolites (**1-6**) were screened for phytotoxic, antifungal, antioomycetes and zootoxic activities.

Phytotoxicity was determined using the leaf puncture bioassay and evaluated on *Phaseolus vulgaris* L., *Quercus suber* L., and *Juglans regia* L. leaves. None of the compounds, except **2**, were active in this bioassay at concentration of 1 mg/mL. Specifically, sphaeropsidin A (**2**) caused necrotic lesions on all plant species tested with area lesion sizes of 75.6 mm^2 on *P. vulgaris* L., 163.3 mm^2 on *J. regia* L. and 15.1 mm^2 on *Q. suber* L.

The antifungal activity of the isolated compounds was tested on two plant pathogenic fungi (*Athelia rolfsii* and *Diplodia corticola*), whereas the antioomycetes activity was evaluated on *Phytophthora cambivora* and *P. lacustris* at concentration of 0.2 mg/plug. PCNB and Metalaxyl-M were used as positive controls depending on the species. Of all the metabolites assayed,

sphaeropsidin A (**2**) inhibited the mycelial growth of all plant pathogens tested (100% inhibition rate). Diplopimarane (**4**) completely inhibited *Athelia rolfsii* and showed, to some extent, good activity against the other three species (*D. corticola*, *P. cambivora* and *P. lacustris*) with inhibition rate ranging from 56.3 % to 74.7%. No colony growth inhibition was observed with the other compounds at the concentration used.

Additionally, the compounds **1**-**6** were screened for lethality in the brine shrimp (*Artemia salina* L.) larvae bioassay, which is widely used for toxicology and ecotoxicology studies. All metabolites were tested at concentration of 100 µg/mL. Compounds **1**, **4** and **6** caused 100% larval mortality. Compound **2** caused 51.3% larval mortality, whereas compounds **3** and **5** were inactive.

Cleistanthane-type diterpenoids are produced by different fungal and plant species but few examples are available on cleistanthane *nor*-diterpenoids as aspergiloids A, B, F and G isolated from the fermentation broth extract of *Aspergillus* sp. YXf3, an endophytic fungus from *Ginkgo biloba*. However, no biological activities were reported for these compounds [26,27].

Sphaeropsidins A, C and G, as well as the other ones B, D-F previously isolated from *D. cupressi, Diplodia mutila* [28] and *D. corticola* [2] belonging to the group of tricyclic and tetracyclic unarranged pimarane diterpenoids are well-known as fungal and plant metabolites [29]. Smardesines and chenopodolins belong also to the same group. These compounds were isolated as cytotoxic and phytotoxic metabolites from *Smardaea* sp. AZ0432 living in the moss *Ceratodon purpureus* [30] and *Phoma chenopodiicola*, a fungus proposed for the biocontrol of *Chenopodoium album* [31,32]. Sphaeropsidin A and its 6-*O*-acetyl derivative also showed interesting antimicrobial [33] and anticancer activity [2,34,35].

Melleins are 3,4-dihydroisocoumarins mainly produced by many fungi of various genera but also by plants, insects and bacteria. They possess several biological activities as phytotoxic, zootoxic and antifungal effects [36]. (-)-Mellein was toxic on grapevine leaves and grapevine calli [2,37,38] and was detected in symptomatic and asymptomatic wood samples and in green shoots [37] on grapevines showing Botryosphaeria dieback and leaf stripe disease. Its role in pathogenesis

was investigated by examining the extent to which it caused the expression of defense-related genes in grapevine calli [38]. Recently, (-)-mellein was also identified as a metabolites of *Lasiodiplodia euphorbiaceicola* during a screening of phytotoxic metabolites isolated from some Lasiodiplodia spp. infecting grapevine in Brazil [17] and from *Sardiniella urbana*, a pathogen found on declining European hackberry trees in Italy [39].

Conclusion

This study represents the first investigation on the secondary metabolites produced by *D. olivarum*, a new emerging pathogen of forest trees in the Mediterranean region. Our findings confirm that *Botryosphaeriaceae* represent an important source of bioactive secondary metabolites some of which with a high application potential in various biotechnology sectors.

Among the metabolites produced *in vitro* by *Diplodia olivarum*, sphaeropsidin A and diplopimarane inhibited the vegetative growth of plant pathogens belonging to different *phyla*. Additionally, the strong activity of the new identified metabolite, olicleistanone (**1**), against *Artemia salina* L. deserves detailed investigations considering that several applications of *A. salina* to toxicology and ecotoxicology continue to be used widely.

Experimental

General experimental procedures

Optical rotations were measured in MeOH on a P-1010 digital polarimeter (Jasco, Tokyo, Japan), unless otherwise note. IR spectra were recorded as deposit glass film on a 5700 FT-IR spectrometer (Jasco, Tokyo, Japan) and UV spectra were measured in MeCN on a V-530 spectrophotometer (Easton, MD, U.S.A.); ^{1}H and ^{13}C NMR spectra were recorded at 400 and 100 MHz in $CDCl_3$ on Bruker spectrometer (Billerica, MA, U.S.A.). The same solvent was used as internal standard. The multiplicities were determined by DEPT spectrum [23]. COSY, HSQC,

HMBC and NOESY spectra were recorded using Bruker microprograms. HR ESIMS spectra were recorded on a 6120 Quadrupole LC/MS instrument (Agilent Technologies, Milan, Italy). Analytical and preparative TLC were performed on silica gel (Kieselgel 60, F_{254}, 0.25 and 0.5 mm respectively) and on reversed phase (Kieselgel 60 RP-18, F_{254}, 0.20 mm) plates (Merck, Darmstadt, Germany). The spots were visualized by exposure to UV radiation (253 nm), or by spraying first with 10% H_2SO_4 in MeOH and then with 5% phosphomolybdic acid in EtOH, followed by heating at 110 °C for 10 min. Column chromatography was performed using silica gel (Merck, Kieselgel 60, 0.063–0.200 mm).

Fungal strain

The *D. olivarum* strain used in this study was originally isolated from a cankered branch of lentisk collected in a natural area on Caprera Island (Italy). Representative sequences were deposited in GenBank, accession number: (ITS: KX833078), (*tef1-α*: KX833079) and (MAT1-2-1: MG015783) [40]. Pure cultures were maintained on potato-dextrose agar (PDA) (Fluka, Sigma-Aldrich Chemic GmbH, Buchs, Switzerland) and stored at 4 °C in the collection of the Dipartimento di Agraria, University of Sassari, Italy, as BL96.

Production, extraction and purification of secondary metabolites

The fungus was grown on two different liquid media (Czapek amended with 2% yeast extract and mineral salt medium [41] both at pH 5.7) in 1L Erlenmeyer flasks containing 250 mL medium. Each flask was seeded with 5 mL of a mycelial suspension and then incubated for 30 d at 25 °C. Culture filtrates were obtained by filtering the culture through filter paper in a vacuum system. The culture filtrate (14.5 L), obtained growing the fungus on Czapek medium, was acidified

to pH 4 with 2 N HCl and extracted exhaustively with EtOAc. The combined organic extracts were dried with Na_2SO_4 and evaporated under reduced pressure. The brown-red oil residue recovered (4.5 g) was fractioned by column chromatography on silica gel (90 × 4 cm) eluted with *n*-hexane-EtOAc (7:3). Eleven fractions were collected and pooled on the basis of similar TLC profiles. Fraction 2 (195.2 mg) was purified by column chromatography on silica gel, eluted with petroleum ether-EtOAc (9.5:0.5), yielding thirteen homogeneous fractions. The residue of the fourth fraction of this latter column (11.0 mg) was further purified by TLC, eluted with *n*-hexane-acetone (8.5:1.5), yielding sphaeropsidin G, **4** [6.7 mg, 0.46 mg/L, R_f 0.82, eluent *n*-hexane-acetone (8.5:1.5)] as an amorphous solid. The residue of the third fraction (103.2 mg) was purified by column chromatography on silica gel (75 × 3 cm), eluted with $CHCl_3$-isoPrOH (93:7), yielding eight homogeneous fractions. The residue of the third fraction of this latter column (23.0 mg) was crystallized with EtOAc-*n*-hexane (1:5) to give diplopimarane, **5** [14.2 mg, 0.97 mg/L, R_f 0.7, eluent *n*-hexane-EtOAc (7:3)] as white crystals. The residue of the eighth fraction (56.4 mg) was purified by preparative TLC, eluted with *n*-hexane-$CHCl_3$-isoPrOH (8:1.5:0.5), yielding olicleistanone (**1**) as an amorphous solid [5.8 mg, 0.4 mg/L, R_f 0.45, eluent *n*-hexane-$CHCl_3$-isoPrOH (8:1.5:0.5)]. The residues of the fifth (290.3 mg) and sixth (278.9 mg) fractions of the first column were combined and crystallized with EtOAc-*n*-hexane (1:5) to give sphaeropsidin A, **2** [312.6 mg, R_f 0.5, eluent *n*-hexane-acetone (7:3), R_f 0.7, eluent *n*-hexane-EtOAc (6:4)] as white crystals. The residue of the seventh fraction (135.1 mg) of the first column was purified by CC on silica gel, eluent *n*-hexane-EtOAc-acetone (6:2.5:1.5), giving sphaeropsidin C, **3** [53.3 mg, 3.67 mg/L, R_f 0.52, eluent *n*-hexane-EtOAc-acetone (6:2.5:1.5), R_f 0.63, eluent *n*-hexane-EtOAc (6:4)] as a white solid, and a further amount of sphaeropsidin A, **2** (33.2 mg, total yield 23.7 mg/L). The culture filtrate (10.0 L), obtained growing the fungus on modified mineral medium, was extracted following the procedure previously described obtaining 3.2 g of organic extract. This latter was fractioned by column chromatography on silica gel (80 × 4 cm) eluted with *n*-hexane-EtOAc (7:3) yielding 10 groups of homogeneous fractions. The residue of the third fraction (302.3 mg) was

purified by column chromatography on silica gel (75 × 3 cm), eluted with *n*-hexane-$CHCl_3$-isoPrOH (7.5:2:0.5), yielding diplopimarane (**5**, 1.4 mg, 0.01 mg/L) and (-)-mellein [**6**, 105.8 mg, 7.30 mg/L, R_f 0.65, eluent *n*-hexane-$CHCl_3$-isoPrOH (7.5:2:0.5)]. The residue of the fourth fraction of the first column (8.2 mg) was further purified by TLC, eluted with *n*-hexane-acetone (8.5:1.5), yielding sphaeropsidin G (**4**, 1.5 mg, 0.10 mg/L). The residue of the fifth (815.9 mg) fraction of the first column was crystallized with EtOAc-*n*-hexane (1:5) to give sphaeropsidin A (**2**, 677 mg, 46.69 mg/L).

Olicleistanone (**1**): UV λ_{max} (log ε) 333 (2.98), 241 (3.55) nm; IR ν_{max} 1725, 1610, 1592, 1560, 1458 cm^{-1}; ^1H and ^{13}C NMR: Table 1; HRESI -MS (+) spectrum *m/z*: 735 $[2M+Na]^+$, 395 $[M+K]^+$, 379.1876 [$C_{22}H_{28}NaO_4$, calcd. 379.1885, $M+Na]^+$, 311 $[M+H-CH_3CH_2OH]^+$.

Sphaeropsidin A (**2**): $[\alpha]_D^{25}$ +104 (*c* 0.4, MeOH); [lit. n.11: $[\alpha]_D^{25}$ +109.6 (*c* 0.2, MeOH); ^1H NMR is very similar to that previously reported [11]; HRESI-MS (+) spectrum *m/z*: 715 $[2M+Na]^+$, 369 $[M+Na]^+$, 347.1820 [$C_{20}H_{27}O_5$, calcd. 347.1780, $M+H]^+$.

Sphaeropsidin C (**3**): $[\alpha]_D^{25}$ +18.3 (*c* 0.7, MeOH); [lit. n. 12: $[\alpha]_D^{25}$ + 16.8 (*c* 1.0, MeOH)]; ^1H NMR is very similar to that previously reported [12]; HRESI-MS (+) spectrum *m/z*: 703 $[2M+K]^+$, 687 $[2M+Na]^+$, 665 $[2M+H]^+$, 333.2037 [$C_{20}H_{29}O_4$, calcd. 333.2066, $M+H]^+$.

Sphaeropsidin G (**4**): $[\alpha]_D^{25}$ +48.6 (*c* 0.8, $CHCl_3$) [lit. n. 16: $[\alpha]_D^{25}$ +51.4 (*c* 0.56, $CHCl_3$)]; ^1H NMR is very similar to that previously reported [16]; ESI-MS (+) spectrum *m/z*: 309 $[M+K]^+$, 293 $[M+Na]^+$, 271 $[M+H]^+$.

Diplopimarane (**5**): $[\alpha]_D^{25}$ +23.0 (*c* 0.10, $CHCl_3$) [lit. n. 14: $[\alpha]_D^{25}$+25.8 (*c* 0.6, $CHCl_3$)]; ^{1}H NMR is very similar to that previously reported [14]; ESIMS (+) spectrum *m/z*: 623 $[2M - 4H + Na]^+$, 339 $[M - 2H + K]^+$, 325 $[M + Na]^+$, 323 $[M - 2H + Na]^+$.

(-)-Mellein (**6**): $[\alpha]^{25}$D -93.0 (*c* 0.3 MeOH) [lit. n. 18: $[\alpha]^{25}_D$ -90 (*c* 0.2, CH_3OH)]; ^{1}H NMR is very similar to that previously reported [18]; ESI MS (+) spectrum *m/z*: 179 $[M + H]^+$.

Computational methods

Molecular mechanics, Hartree-Fock (HF) and density functional theory (DFT) calculations were run with Spartan'18 (Wavefunction, Inc., Irvine CA, 2018), with standard parameters and convergence criteria. First, the conformers of (7*S*,15*S*)-**1** and (7*S*,15*R*)-**1** were investigated with the Monte Carlo algorithm using Merck molecular force field (MMFF).

They were then screened by geometry optimizations at HF/3-21G level, single-point calculations at B3LYP/6-31G(d) level, and final geometry optimizations at the same level. Energies and populations were then estimated at the B97M-V/6-311+G(2df,2p) level. The procedure afforded 6 energy minima for (7*S*,15*S*)-**1** and 10 minima for (7*S*,15*R*)-**1** within the final energy threshold (10 kJ/mol at B97M-V/6-31G(d) level). ^{13}C-NMR chemical shifts were then calculated with the GIAO method at ωB97X-D/6-31G(d) level. An empirical correction was applied depending on the number of bonds to the carbon and on the bond lengths [24]. ^3J coupling constants were as Boltzmann averages of all DFT structures described above, either with a Karplus equation or at B3LYP/pcJ-0 level (Fermi contact term only).

Leaf puncture assay

Phaseolus vulgaris L, *Juglans regia* L. and *Quercus suber* L. leaves were used for this assay. Each compound was tested at 1.0 mg/mL. The assay was performed as previously reported [14]. Each treatment was repeated three times. Leaves were observed daily and scored for symptoms

after 5 days. The effect of the toxins on the leaves was observed up to 10 days. Lesions were estimated using APS Assess 2.0 software following the tutorials in the user's manual. The lesion size was expressed in mm^2.

Antifungal assays

All compounds (**1-6**) were preliminarily tested on four different plant pathogens including two fungal species (*Athelia rolfsii* and *Diplodia corticola)* and two *oomycetes* (*Phytophthora cambivora* and *P. lacustris*). The sensitivity of all species to these compounds was evaluated, depending on the species, on CA (carrot agar medium) or PDA (potato dextrose agar) as inhibition of the mycelial radial growth. The assay was performed as previously reported [42]. Each metabolite was tested at 200 μg/plug. Methanol was used as negative control. Metalaxyl-M (mefenoxam; p.a. 43.88%; Syngenta), a synthetic fungicide to which the oomycetes are sensitive, and PCNB (pentachloronitrobenzene) for ascomycetes and basidiomycetes, were used as positive control. Each treatment consisted of three replicates and the experiment was repeated twice.

Artemia salina bioassay

All compounds were assayed on brine shrimp larvae (*Artemia salina* L.). The assay was performed in cell culture plates with 24 cells (Corning) as previously described [14. The metabolites were tested at 100 μg/mL. Tests were performed in quadruplicate. The percentage of larval mortality was determined after 36 h incubation at 27 °C in the dark.

Supporting Information

1D and 2D NMR data for **1** and HRESI-MS spectra of **1-3**.

Acknowledgements

Antonio Evidente is associated with the Istituto di Chimica Biomolecolare del CNR, Pozzuoli, Italy.

ORCID® iDs

Marco Masi: 0000-0003-0609-8902

Gennaro Pescitelli: 0000-0002-0869-5076

Lucia Maddau: 0000-0002-8158-8242

Antonio Evidente: 0000-0001-9110-1656

Roberta Di Lecce: 0000-0002-8797-6406

Benedetto Teodoro Linaldeddu: 0000-0003-2428-9905

References

1. Alves, A.; Linaldeddu, B. T.; Deidda, A.; Franceschini. A. Fungal Divers. **2014**, *67*, 143–156.
2. Masi, M.; Maddau, L.; Linaldeddu, B. T.; Scanu, B.; Evidente, A.; Cimmino, A. *Curr. Med. Chem.* **2018**, *25*, 208–252.
3. Pérez, C.; Wingfield, M.; Slippers, B.; Altier, N.; Blanchette R. *Fungal Divers.* **2010**, *41*, 53–69.
4. Adamson, K.; Klavina, D.; Drenkhan, R.; Gaitnieks, T.; Hanso, M. *Eur. J. Plant Pathol.* **2015**, *143*, 343–350.
5. Martin, D. K. H.; Turcotte, R. M.; Miller, T. M.; Munck, I. A.; Aćimović, S. G.; Macias, A. M.; Stauder, C. M.; Kasson, M. T. *Plant Dis.* **2017**, *101*, 380.
6. Cimmino, A.; Maddau, L.; Masi, M.; Linaldeddu, B. T.; Pescitelli, G.; Evidente, A. *Chem. Biodivers.* **2017a**, *14*, e1700325.
7. Lazzizera, C.; Frisullo, S.; Alves, A.; Lopes, J.; Phillips, A. J. L. *Fungal Divers.* **2008**, *31*, 63–71.

8. Granata, G.; Faedda, R.; Sidoti, A. *Plant Dis.* **2016**, *100*, 2483–2491.
9. Linaldeddu, B. T.; Maddau, L.; Franceschini, A.; Alves, A.; Phillips A. J. L. *Mycosphere* **2016**, *7*, 962–977.
10. Manca, D.; Bregant, C.; Maddau, L.; Pinna, C.; Montecchio, L.; Linaldeddu, B. T. *Ital. J. Mycol.* **2020**, 49, 85–91.
11. Evidente, A.; Sparapano, L.; Motta, A.; Giordano, F.; Fierro, O.; Frisullo, S. *Phytochemistry* **1996**, *42*, 1541–1546.
12. Evidente, A.; Sparapano, L.; Fierro, O.; Bruno, G.; Giordano, F.; Motta, A. *Phytochemistry* **1997,** *45*, 705–713.
13. Evidente, A.; Punzo, B.; Andolfi, A.; Cimmino, A.; Melck, D.; Luque, J. *Phytopathol. Mediterr.* **2010**, *49*, 74–79.
14. Andolfi, A.; Maddau, L.; Basso, S.; Linaldeddu, B. T.; Cimmino, A.; Scanu, B.; Deidda, A.; Tuzi, A.; Evidente, A. *J. Nat. Prod.* **2014**, *77*, 2352–236.
15. Abou-Mansour, E.; Débieux, J. L.; Ramírez-Suero, M.; Bénard-Gellon, M.; Magnin-Robert, M.; Spagnolo, A.; Serrano, M. *Phytochemistry* **2015**, *115*, 207–215.
16. Cimmino, A.; Maddau, L.; Masi, M.; Evidente, M.; Linaldeddu, B. T.; Evidente, A. *Tetrahedron* **2016**, *72*, 6788–6793.
17. Cimmino, A.; Cinelli, T.; Masi, M.; Reveglia, P.; da Silva, M. A.; Mugnai, L.; Evidente, A. *J. Agric. Food Chem.* **2017b**, *65*, 1102–1107.
18. Masi, M.; Aloi, F.; Nocera, P.; Cacciola, S.O.; Surico, G.; Evidente, A. *Toxins* **2020**, *12*, 126.
19. Devappa, R. K.; Makkar, H. P.; Becker, K. *J. Am. Oil Chem. Soc.* **2011**, *88*, 301–322.
20. Breitmaier, E.; Voelter, W. *Carbon-13 NMR Spectroscopy*. VCH, Weinheim, Germany, 1987; pp. 183–280.
21. Nakanishi, K.; Solomon, P. H. *Infrared Absorption Spectroscopy*, 2nd ed.; Holden Day: Oakland, California, USA, 1977; pp 17−44.

22. Pretsch, E.; Bühlmann, P.; Affolter, C. Structure Determination of Organic Compounds – Tables of Spectral Data, 3rd ed.; Springer-Verlag: Berlin, Germany, 2000; pp. 161–243.
23. Berger, S.; Braun, S. *200 and More Basic NMR Experiments: A Practical Course*, 1st ed.; Wiley-VCH, Weinheim, Germany, 2004.
24. Hehre, W.; Klunzinger, P.; Deppmeier, B.; Driessen, A.; Uchida, N.; Hashimoto, M.; Fukushi, E.; Takata, Y. *J. Nat. Prod.* **2019**, *82*, 2299−2306.
25. Zask, A.; Ellestad, G. *Chirality* **2018**, *30*, 157−164.
26. Guo, Z. K.; Yan, T.; Guo, Y.; Song, Y. C.; Jiao, R. H.; Tan, R. X.; Ge, H. M. *J. Nat. Prod.* **2012**, *75*, 15−21.
27. Yan, T.; Guo, Z. K.; Jiang, R.; Wei, W.; Wang, T.; Guo, Y.; Song, Y. C.; Jiao, R. H.; Tan, R. X.; Ge, H. M. *Planta Med.* **2013**, *79*, 348−352.
28. Sparapano, L.; Bruno, G.; Fierro, O.; Evidente, A. *Phytochemistry* **2004**, *65*, 189−198.
29. Reveglia, P.; Cimmino, A.; Masi, M.; Nocera, P.; Berova, N.; Ellestad, G.; Evidente, A. *Chirality* **2018**, *30*, 1115−1134.
30. Wang, X. N.; Bashyal, B. P.; Wijeratne, E. K.; U'Ren, J. M.; Liu, M. X.; Gunatilaka, M. K.; Arnold, A. E.; Gunatilaka, A. L. *J. Nat. Prod.* **2011**, *74*, 2052−2061.
31. Cimmino, A.; Andolfi, A.; Zonno, M. C.; Avolio, F.; Santini, A.; Tuzi, A.; Berestetskiy, A.; Vurro, M.; Evidente, A. *J. Nat. Prod.* **2013**, *76*, 1291−1297.
32. Evidente, M.; Cimmino, A.; Zonno, M. C.; Masi, M.; Berestetskyi, A.; Santoro, E.; Superchi, S.; Vurro, M.; Evidente, A. *Phytochemistry* **2015**, *117*, 482−488.
33. Evidente, A.; Venturi, V.; Masi, M.; Degrassi, G.; Cimmino, A.; Maddau, L.; Andolfi, A. *J. Nat. Prod.* **2011**, *74*, 2520−2525.
34. Lallemand, B.; Masi, M.; Maddau, L.; De Lorenzi, M.; Dam, R.; Cimmino, A.; Moreno y Banuls, L.; Andolfi, A.; Kiss, R.; Mathieu, V.; Evidente, A. *Phytochem. Lett.* **2012**, *5*, 770−775.

35. Ingels, A.; Dinhof, C.; Garg, A. D.; Maddau, L.; Masi, M.; Evidente, A.; Berger, W.; Dejaegher, B.; Mathieu, V. *Cancer Chemoth. Pharm.* **2017**, *79*, 971−983.
36. Reveglia, P.; Masi, M.; Evidente, A. *Biomolecules* **2020**, *10*, 772.
37. Djoukeng, J. D.; Polli, S.; Larignon, P.; Abou-Mansour, E. *Eur. J. Plant Pathol.* **2009**, *124*, 303−308.
38. Ramírez-Suero, M.; Bénard-Gellon, M.; Chong, J.; Laloue, H.; Stempien, E.; Abou-Mansour, E.; Bertsch, C. *Protoplasma* **2014**, *251*, 1417−1426.
39. Cimmino, A.; Maddau, L.; Masi, M.; Linaldeddu, B. T.; Evidente, A. *Nat. Prod. Res.* **2019**, *33*, 1862−1869.
40. Lopes, A.; Linaldeddu, B. T.; Phillips, A. J. L.; Alves, A. *Fungal Biol.* **2018**, *122*, 629−638.
41. Pinkerton, F.; Strobel, G. *PNAS* **1976**, *73*, 4007−4011.
42. Masi, M.; Maddau, L.; Linaldeddu, B. T.; Cimmino, A.; D'Amico, W.; Scanu, B.; Evidente, M.; Tuzi, A.; Evidente, A. *J. Agric. Food Chem.* **2016**, *64*, 217−225.

Table 1: ^{1}H and ^{13}C NMR and HMBC data of olicleistanone (**1**)[a,b]

position	δ_C[c]	δ_H (*J* in Hz)	HMBC
1	27.4 t	2.77 (1H) dt (18.8, 6.1)	H_2-2, H_2-3
		2.47 (1H) ddd (18.8, 12.2, 6.6)	
2	18.6 t	1.80 m (2H)	H_2-1
3	40.5 t	1.62 (1H) m	H_2-1, H_2-2, H_3-18, H_3-19
		1.49 (1H) m	
4	34.0 s		H_2-2, H_2-3, H_3-18, H_3-19
5	136.4 s		H_2-1, H_2-3, H_3-18, H_3-19
6	195.5 s		H_2-1
7	92.3 s		H-15, H_2-16, H-20A
8	130.6 s		H-12, H_3-17
9	132.9 s		
10	146.1 s		H_2-1, H_2-2, H-11
11	125.0 d	7.31 (1H) d (7.9)	
12	131.3 d	7.18 (1H) d (7.9)	
13	138.7 s		H-11, H_3-17
14	130.2 s		H-12, H-15, H_2-16
15	69.5 d	4.20 (1H) d (3.3)[e]	H_2-16, H_3-22
16	60.5 t	4.22 (1H) dd (12.7, 3.3)[e]	H-15
		4.41 (1H) d (12.7)	
17	18.4 q	2.34 (3H) s	H-12
18[d]	27.7 q	1.23 (3H) s	H_3-19
19[d]	29.7 q	1.36 (3H) s	H_3-18
20	59.0 t	3.33 (1H) dq (14.2, 7.0)	H_3-21
		3.64 (1H) dq (14.2, 7.0)	
21	15.4 q	1.14 (3H) t (7.0)	
22	55.7 q	3.38 (3H) s	H-15

[a]2D ^{1}H, ^{1}H (COSY) and ^{13}C, ^{1}H (HSQC) NMR experiments confirmed the correlations of all the protons and the corresponding carbons. [b]Coupling constants (*J*) are given in parenthesis. [c]Multiplicities were assigned with DEPT. [d]These signals could be exchanged. [e] These two signals are in part overlapped.

Table 2: NOESY data of olicleistanone

Irradiated	Observed	Irradiated	Observed
H-11	H_2-1	OMe	H_3-17
H_2-20	H_3-21	H_3-18	H_2-20
H-15	H_3-17, OMe		

Table 3: Experimental and calculated $^3J_{HH}$ values (Hz) of olicleistanone[a]

	Experimental	Calculated (Karplus)	Calculated (DFT)	Calculated (Karplus)	Calculated (DFT)
		(7*S*,15*S*)-**1**		(7*S*,15*R*)-**1**	
H-15/H-16a	3.3	3.14	4.05	7.24	9.26
H-15/H-16b	not detected	0.89	0.7	7.81	8.63

[a] *J* values calculated either by a Karplus curve or by DFT at B3LYP/pcJ-0 level in vacuo, as Boltzmann average of all structures obtained by DFT geometry optimization (see text).

Figure Legend

Figure 1. Foliar symptoms on lentisk shoots infected by *D. olivarum*.

Figure 2. Structures of olicleistanone (**1**), sphaeropsidins A, C and G (**2-4**), diplopimarane (**5**) and (-)-mellein (**6**).

Figure 1.

Figure 2.

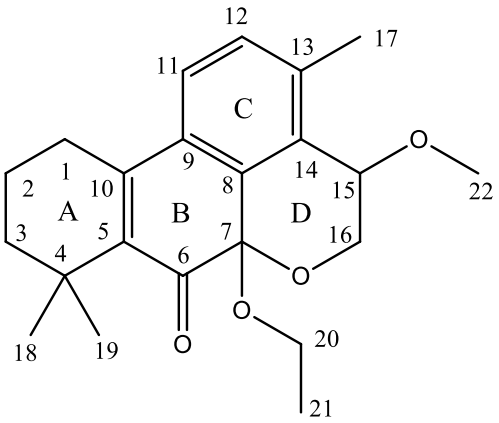

1, Olicleistanone

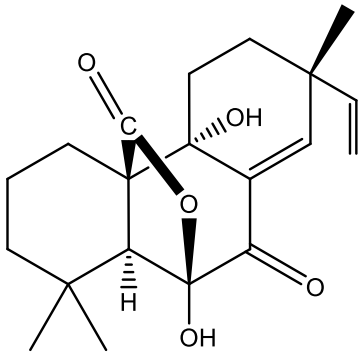

2, Sphaeropsidin A

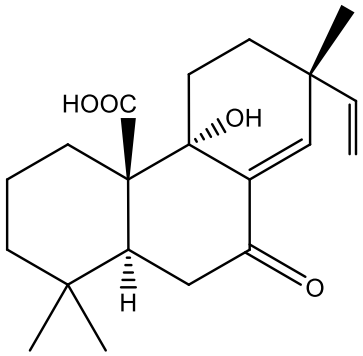

3, Sphaeropsidin C

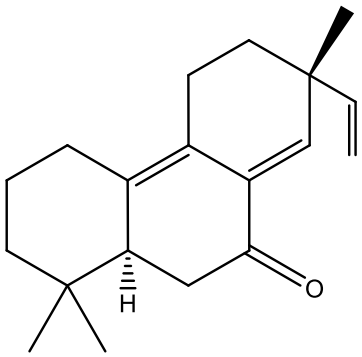

4, Sphaeropsidin G

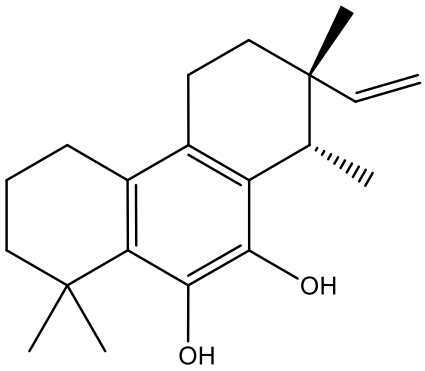

5, Diplopimarane

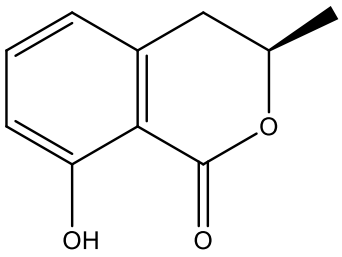

6 (-)-Mellein